Available online at www.sciencedirect.com
SCIENCE DIRECT®
Journal of Solid State Chemistry 178 (2005) 892–896
JOURNAL OF SOLID STATE CHEMISTRY
www.elsevier.com/locate/jssc

High-resolution transmission electron microscopy investigation of nanostructures in SnO_2 thin films prepared by pulsed laser deposition

Z.W. Chen*, J.K.L. Lai, C.H. Shek

Department of Physics and Materials Science, City University of Hong Kong, 83 Tat Chee Avenue, Kowloon Tong, Hong Kong, SAR, People's Republic of China

Received 29 November 2004; received in revised form 10 January 2005; accepted 15 January 2005

Abstract

Pulsed laser deposition (PLD) was used to grow nanocrystalline SnO_2 thin films onto glass substrates. The nanocrystallites and microstructures in SnO_2 thin films grown by PLD techniques have been investigated in detail by using X-ray diffraction and high-resolution transmission electron microscopy (HRTEM). The PLD process was carried out at room temperature under a working pressure of about 2×10^{-6} mbar. Experimental results indicate that thin films are composed of a polycrystalline SnO_2 and an amorphous SnO phase. In particular, the presence of such an amorphous SnO phase in the thin films greatly limits their practical use as gas-sensing devices. HRTEM observations revealed that SnO_2 nanocrystallites with tetragonal rutile structure embed in an amorphous SnO matrix, which are approximatively equiaxed. These approximatively equiaxed SnO_2 nanocrystallites contain a high density of defects, such as twin boundaries and edge dislocations. The grain growth of SnO_2 thin films may be discussed in terms of the coalescent particle growth mechanism.

Keywords: SnO_2 thin film; Microstructure; Nanocrystallite; Pulsed laser deposition

1. Introduction

The microstructural evolution of tin dioxide (SnO_2) thin films has been studied exhaustively and this topic has recently gained even greater importance due to the interest in controlling particle size in nanostructured materials [1–7]. Moldovan et al. [3] have used analytical and simulation methods to characterize the growth law and morphology of two-dimensional growth by grain-rotation-induced grain coalescence in polycrystalline microstructures. Leite et al. [5] reported on experimental evidence indicating that the crystal growth process took place in a colloidal nanocrystal system at room temperature. This crystal growth process is based on grain rotation among neighboring grains, resulting in a coherent grain–grain interface, which, by eliminating common boundaries, causes neighboring grains to coalesce, thereby forming a single larger nanocrystal. With the continuous breakdown of sizes and the increased demand on performance for optical, electronic, and magnetic devices, the control of thin film structures is becoming increasingly significant. Many efforts have been devoted to investigation of the growth mode [8,9], to the formation of crystallographic structures [10,11], and to the kinetic morphology evolution of island ensembles [12,13]. SnO_2 is widely employed in gas-sensing applications because of its excellent response to different pollutant gases [14]. Under a nanostructured form, the nanocrystalline SnO_2 thin films have been shown to exhibit better gas-sensing performance than their micro- and/or macro-structured counterparts [15]. Therefore, the investigation of the micro- and nanostructure characteristics of SnO_2 thin films, by means of X-ray diffraction (XRD) and high-resolution transmission electron microscopy

*Corresponding author. Fax: +852 2788 7830
E-mail address: cnzwchen@yahoo.com.cn (Z.W. Chen).

0022-4596/$ - see front matter © 2005 Elsevier Inc. All rights reserved.
doi:10.1016/j.jssc.2005.01.013

(HRTEM) [16,17], is an essential step toward a better understanding of how the growth conditions influence the thin film nanostructure which, in turn, determines the film sensing performance. In this context, the pulsed laser deposition (PLD) technique stands out by its unique features, such as its extremely high instantaneous deposition rate and the highly energetic ablated species, that permit the growth of nanostructured thin films exhibiting unprecedented properties [18].

In this paper, we report on an HRTEM investigation of nanostructures of SnO_2 thin films prepared by PLD. Experimentally, PLD deposition under vacuum is found to produce thin films that are composed of both a polycrystalline SnO_2 phase and an amorphous SnO phase. HRTEM observations revealed that the SnO_2 nanocrystallines with tetragonal rutile structure are embed in an amorphous SnO matrix, and tend to be approximatively equiaxed. These approximatively equiaxed SnO_2 nanocrystallites contain a high density of defects, such as twin boundaries and edge dislocations. The grain growth of SnO_2 thin films may be discussed in terms of the coalescent particle growth mechanism.

2. Experimental

SnO_2 thin films were prepared by the PLD method [17]. Sintered cassiterite SnO_2 bulk was used as the target. The circular target consisted of a high-purity commercial SnO_2 (99.8%) disk. The size of the target was about $\varnothing 15\,\text{mm} \times 4\,\text{mm}$, and they were installed to minimize contamination. The laser was a KrF excimer laser producing pulse energies of 350 mJ at a wavelength of 248 nm, and the duration of every excimer laser pulse was 34 ns. The laser energy was deposited onto the target in a high-vacuum chamber through a UV-grade fused silica window using a UV-grade fused silica lens. During the experiment, the laser was operated at a repetition rate of 10 Hz at an incident angle of 45° to the polished sintered cassiterite SnO_2 target, which was rotating at a rate of 15 rpm to avoid drilling. The fluence was set at about $5\,\text{J/cm}^2$ per pulse, with a total of approximately 150,000 laser pulses. The growth rate was estimated to be about 0.3 nm/s (or 1 μm/h) and the final as-deposited thin film thickness was about 4 μm. The ablated substance was collected on a glass slide, which was mounted on a substrate holder 2.5 cm away from the target. The high vacuum in the deposition chamber was achieved using a cryopump. The base pressure prior to laser ablation was about 1×10^{-6} mbar, and the working pressure during laser ablation was about 2×10^{-6} mbar. All deposition processes were carried out at ambient temperature.

XRD patterns were recorded at a scanning rate of 0.05°/s in the 2θ range from 15° to 65° using a *Philips X'pert* diffractometer with Cu $K\alpha$ radiation (1.5406 Å), reflection geometry, and proportional counter. The nanocrystallite quality of the SnO_2 thin films was characterized using high-resolution observation of the microstructural evolution of SnO_2 nanoclusters, which were performed using a JEOL-2010 transmission electron microscope (HRTEM), with a point-to-point resolution 1.94 Å, operated at 200 kV.

3. Results and discussion

Figs. 1a and b show XRD patterns of the cassiterite SnO_2 bulk and the as-prepared SnO_2 thin films, respectively. All reflections can be indexed with tetragonal cell of SnO_2, and all cell parameters are close to $a = 4.737$ Å, and $c = 3.185$ [19]. The SnO_2 average sizes were calculated using the Scherrer formula: $D = K\lambda/\beta \cos\theta$, where D is the diameter of the nanoparticles, $K = 0.9$, $\lambda(\text{Cu}K\alpha) = 1.5406$ Å, and β is the full-width at half-maximum of the diffraction lines. XRD results show that the average grain size of the as-prepared nanocrystalline SnO_2 is about 12 nm. The

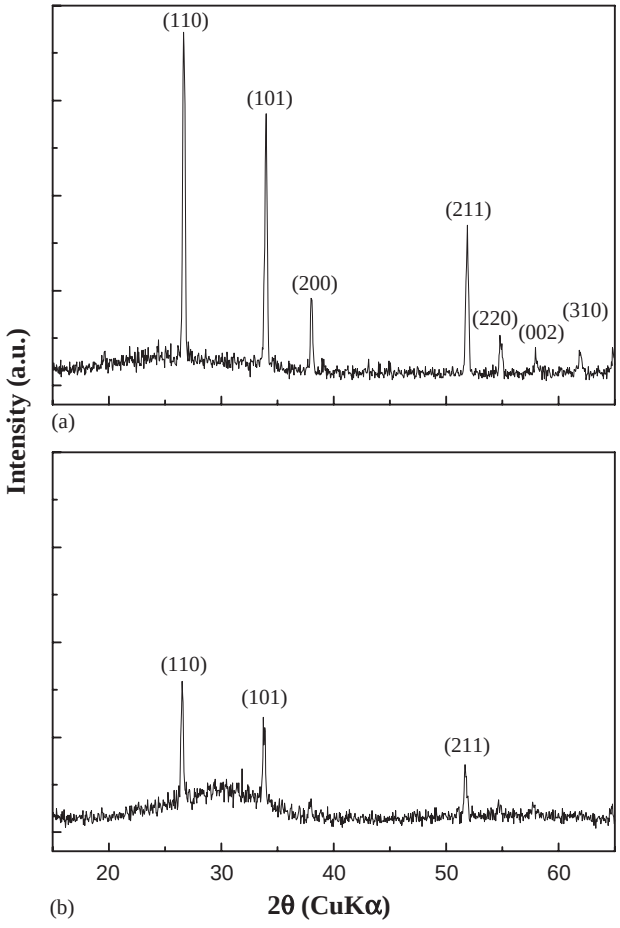

Fig. 1. XRD patterns of SnO_2: (a) SnO_2 bulk material and (b) as-prepared SnO_2 thin film.

crystallographic planes identified on the XRD patterns presented in Fig. 1b are indeed typical of a pure polycrystalline SnO_2 phase, in terms of peak positions and relative peak intensities [20]. However, we noted that a broad peak centered around $2\theta = 30^\circ$ is clearly visible in the XRD pattern of the PLD SnO_2 thin films (see Fig. 1b). We believe that this broad peak is due to the presence of an amorphous SnO phase. This has been clearly demonstrated in previous work [21], where PLD SnO_2 thin films grown under vacuum (laser fluence of $\sim 4.6\,J/cm^2$), over a wide range of deposition temperatures (from room temperature to 600 °C), were shown to consist of both a polycrystalline SnO_2 phase and an amorphous SnO (*a*-SnO) phase. Our experimental result is also supported by the existing literature on the deposition by PLD of SnO_2 thin films, in which films deposited under vacuum were always found to exhibit both poly-SnO_2 and *a*-SnO phases [22–25]. It is worth recalling that such a lack of oxygen in the deposited films is known to result from laser-induced oxygen desorption from the surface layers of the SnO_2 target [23], leading thereby to the growth of a nonstoichiometric compound. The XRD signature of *a*-SnO is a broad component centered around $2\theta = 29.8^\circ$, which corresponds to the most intense reflection of the SnO phase [26], in agreement with the XRD patterns shown in Fig. 1b. Moreover, for PLD SnO_2 thin films as thick as 4 μm (in our experiment), more than 98% of the XRD signal originates from the film, eliminating thereby any relevant discussion about a possible contribution of the glass substrate to the broad component of the XRD pattern shown in Fig. 1b. In any case, the broad peak that characterizes glass is known to be centered near $2\theta = 26^\circ$. The presence, therefore, of such an amorphous SnO phase in the films suggests that the growth conditions (i.e., under vacuum at room temperature) are in fact not appropriate for a complete crystallization of the pure SnO_2 phase. This conclusion agrees with previous results [21], where it was demonstrated that an oxygen background pressure is a prerequisite for the growth of pure polycrystalline SnO_2 phase.

In order to explain the nanostructures of the SnO_2 nanocrystallites, we should investigate the possible mechanism to explain the microstructural behavior. This is what we attempt to do in this paper. HRTEM investigation of the SnO_2 thin films, which can be used as elements of conductance sensors, can give useful information about local composition at dislocation cores. Fig. 2 shows a low-magnification HRTEM image and the selected area electron diffraction (SAED) pattern (inset) of the as-prepared SnO_2 thin film prepared by the PLD method. In our XRD pattern, we have noted that the intensity of the diffraction peaks on the XRD pattern of the as-prepared thin films (see Fig. 1b) is lower than that of the bulk material. In fact, this observation may be simply indicative of a lower

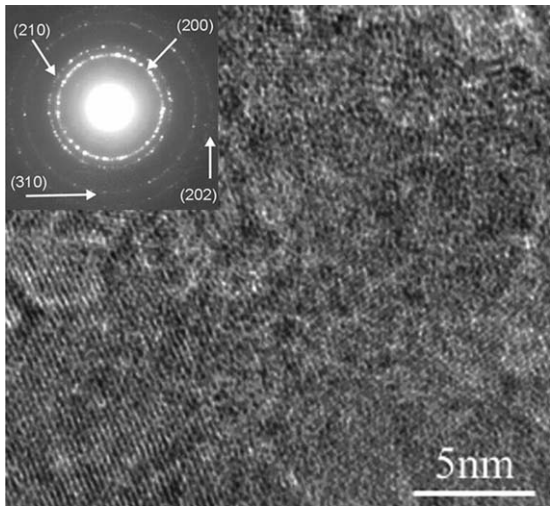

Fig. 2. A high-resolution transmission electron micrograph and SAED pattern (inset) of the as-prepared SnO_2 thin film prepared by PLD method.

degree of crystallinity of the as-prepared thin films as they contain an amorphous SnO phase. As seen in the HRTEM image, we found that amorphous SnO matrix contains randomly, small crystallites with many micropores. The lattice fringes of nanocrystalline SnO_2 were clearly visible. Moreover, these nanocrystallites are approximatively equiaxed. The contrast of the particles in different regions of the HRTEM image indicates a different density, which may be related to the grain sizes. The polycrystalline diffraction rings of the SAED pattern (inset in Fig. 2) also demonstrate the microstructural characteristics of the typical tetragonal SnO_2 thin films ($d_{200} = 2.37\,Å$, $d_{210} = 2.12\,Å$, $d_{310} = 1.50\,Å$, and $d_{202} = 1.32\,Å$). However, it is necessary to point out that the (110) and (101) diffraction rings are surprisingly absent from the SAED pattern presented in inset of Fig. 2. This is particularly intriguing when one notices that (110) and (101) planes are identified in the HRTEM image [17]. In fact, the (110) and (101) diffraction rings are always clearly visible on SAED patterns of SnO_2 thin films regardless of their deposition method, either PLD or sputtering. In the inset of Fig. 2, we believe that the broad and intense central spot hinders observation where the missing rings are expected to appear. Moreover, such a large and diffuse central spot may be indicative of the presence of an *a*-SnO phase, which is consistent with the previous results [21].

Figs. 3a and b show additional high-resolution transmission electron micrographs of the as-prepared SnO_2 thin films prepared by PLD method. As seen in Fig. 3, besides the amorphous SnO phase, several nanocrystallites are clearly visible. In Fig. 3a, we found that the SnO_2 nanoparticle is clearly crystalline with the approximatively equiaxed (see two white rounds A and B). However, the nanocrystalline SnO_2 grains are often

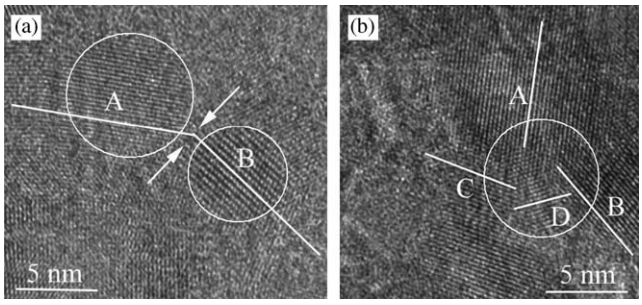

Fig. 3. High-resolution transmission electron micrographs of the as-prepared SnO_2 thin films prepared by the PLD method.

overlapped and connected with two or three neighbors through necks in the as-prepared SnO_2 thin films (see white arrows). The overlapped parts show more edge dislocations in the as-prepared SnO_2 thin film. In Fig. 3b, besides the nanocrystallites A and B, we found that the nanocrystalline SnO_2 grains are overlapped and connected with four neighbors through necks in the as-prepared SnO_2 thin film (see A, B, C, and D). The overlapped parts contain a high density of defects, such as twin boundaries, shown in the center neighborhood of white circle. The above results indicate that the PLD deposition under vacuum was found to produce thin films that were composed of both a polycrystalline SnO_2 phase and an amorphous SnO phase. In particular, the presence of such an amorphous SnO phase in the thin films greatly limits their practical use as gas-sensing devices. Therefore, there is still a need to identify the optimal growth conditions for PLD SnO_2-based gas sensors.

Since the phenomenon of gas sensitivity is related to electron transport, the geometry and nature of the contact areas between SnO_2 particles is especially important. The grain-rotation process is directly related to the reduction of surface energy, aimed at minimizing the area of high-energy faces [3,4]. Thus, an analysis of the surface energy in several crystallographic orientations can be useful to predict preferential growth directions. Leite et al. [5] have calculated the specific surface energy, and found that the surface energy of the (001) surface is 1.53 times greater than that of the (110) surface, and that of the (101) surface is 1.19 times than that of the (110) surface. Our HRTEM results indicate that, in most cases, the grains predominantly grow with preferred (101)-plane orientation, and connected with two or three neighbors through necks. This is in good agreement with other experimental and theoretical results reported in the literatures [3–5]. These results reveal the formation of primary particle clusters resulting in a single large nanocrystalline, and the clusters grew preferentially in the (101) direction, which occurs on high-surface-energy plane.

4. Conclusions

In conclusion, we report on an HRTEM investigation of nanostructures in SnO_2 thin films prepared by PLD. Experimental results indicate the PLD deposition under vacuum is found to produce thin films that are composed of both a polycrystalline SnO_2 phase and an amorphous SnO phase. HRTEM observations revealed that SnO_2 nanocrystallines, with a tetragonal rutile structure, are embed in an amorphous SnO matrix, and tend to be approximatively equiaxed. These approximatively equiaxed SnO_2 nanocrystallites contain a high density of defects, such as twin boundaries and edge dislocations. The grain growth of SnO_2 thin films was discussed in terms of the coalescent particle growth mechanism.

Acknowledgments

The work described in this paper was fully supported by a grant from the Research Grant Council of Hong Kong Special Administrative, China (Project No. CityU 101303).

References

[1] C.T. Campbell, S.C. Parker, D.E. Starr, Science 298 (2002) 811.
[2] K.L. Merkle, L.J. Thompson, Phys. Rev. Lett. 88 (2002) 225501.
[3] D. Moldovan, V. Yamakov, D. Wolf, S.R. Phillport, Phys. Rev. Lett. 89 (2002) 206101.
[4] R.L. Penn, J.F. Banfield, Science 281 (1998) 969.
[5] E.R. Leite, T.R. Giraldi, F.M. Pontes, E. Longo, A. Beltrán, J. Andrés, Appl. Phys. Lett. 83 (2003) 1566.
[6] E.R. Leite, I.T. Weber, E. Longo, J.A. Varela, Adv. Mater. 12 (2000) 965.
[7] E.R. Leite, A.P. Maciel, I.T. Weber, P.N. Lisboa-Filho, E. Longo, C.O. Paiva-Santos, A.V.C. Andrade, C.A. Paskocimas, Y. Maniette, W.H. Schreiner, Adv. Mater. 14 (2002) 905.
[8] V. Musolino, A. Dal Corso, A. Selloni, Phys. Rev. Lett. 83 (1999) 2761.
[9] M. Hu, S. Noda, H. Komiyama, Surf. Sci. 513 (2002) 530.
[10] S. Bajt, D.G. Steams, P.A. Kearney, J. Appl. Phys. 90 (2001) 1017.
[11] J.M. Soler, M.R. Beltran, K. Michaelian, I.L. Garzon, P. Ordejon, D. Sanchez-Portal, E. Artacho, Phys. Rev. B 61 (2000) 5771.
[12] M. Hu, S. Noda, Y. Tsuji, T. Okubo, Y. Yamaguchi, H. Komiyama, J. Vac. Sci. Technol. A 20 (2002) 589.
[13] J.M. Zuo, B.Q. Li, Phys. Rev. Lett. 88 (2002) 255502.
[14] G. Williams, G.S.V. Coles, J. Mater. Chem. 8 (1998) 165.
[15] L. Bruno, C. Pijolat, R. Lalauze, Sensor Actuator B 18–19 (1994) 195.
[16] A.M. Serventi, R. Dolbec, M.A. El Khakani, R.G. Saint-Jacques, D.G. Rickerby, J. Phys. Chem. Solids 64 (2003) 2097.
[17] Z.W. Chen, J.K.L. Lai, C.H. Shek, H.D. Chen, J. Mater. Res. 18 (2003) 1289.
[18] A.M. Serventi, M.A. El Khakani, R.G. Saint-Jacques, D.G. Rickerby, J. Mater. Res. 16 (2001) 2336.

[19] J.G. Zheng, X.Q. Pan, M. Schweizer, U. Weimar, W. Göpel, M. Rühle, Philos. Mag. Lett. 73 (1996) 93.
[20] Joint Committee for Powder Diffraction Standards (JCPDS) Data Card, 72-1147, International Center of Diffraction Data, Swarthmore, PA, 1995.
[21] R. Dolbec, M.A. El Khakani, A.M. Serventi, M. Trudeau, R.G. Saint-Jacques, Thin Solid Films 419 (2002) 230.
[22] R.D. Vispute, V.P. Godbole, S.M. Chaudhari, S.M. Kanetkar, S.B. Ogale, J. Mater. Res. 3 (1988) 1180.
[23] V.P. Godbole, R.D. Vispute, S.M. Chaudhari, S.M. Kanetkar, S.B. Ogale, J. Mater. Res. 5 (1990) 372.
[24] H.M. Phillips, Y. Li, Z. Bi, B. Zhang, Appl. Phys. A 63 (1996) 347.
[25] R. Lal, R. Grover, R.D. Vispute, R. Viswanathan, V.P. Godbole, S.B. Ogale, Thin Solid Films 206 (1991) 88.
[26] Joint Committee for Powder Diffraction Standards (JCPDS) Data Card, 72-1024, International Center of Diffraction Data, Swarthmore, PA, 1995.